Electronic structure and magnetic properties of naphthalene- and stilbene-diimide-bridged diuranium(V) complexes: a theoretical study

Seddik Boucenina, Lotfi Belkhiri, Samir Meskaldji, Roberto Linguerri, Gilberte Chambaud, Abdou Boucekkine, Majdi Hochlaf

Electronic structure and magnetic properties of naphthalene- and stilbene-diimide-bridged diuranium(V) complexes: A theoretical study

Seddik Boucenina,[a,b] Lotfi Belkhiri,[a,*] Samir Meskaldji,[a,c] Roberto Linguerri,[b] Gilberte Chambaud,[b] Abdou Boucekkine,[d] Majdi Hochlaf [b,*]

[a] Laboratoire de Physique Mathématique et Subatomique LPMS, Département de Chimie, Université des Frères Mentouri, 25017 Constantine, Algeria.

[b] Université Gustave Eiffel, COSYS/LISIS, 5 Bd Descartes 77454, Champs sur Marne, France.

[c] Ecole Normale Supérieure de l'Enseignement Technique - ENSET Skikda 21000, Algeria.

[d] Univ Rennes, UMR 6226 CNRS, Campus de Beaulieu, F-35042 Rennes Cedex, France.

Corresponding authors

*Email (L. Belkhiri): lotfi.belkhiri@umc.edu.dz

*Email (M. Hochlaf): hochlaf@univ-mlv.fr

Abstract

The magnetic exchange coupling between two diuranium(V) ions exhibiting the $5f^1$-$5f^1$ configuration in diimide-bridged complexes $[Cp_3U^V]_2(\mu\text{-L})$ (L = stilbene-, naphthalene-diimide) has been investigated theoretically using relativistic ZORA/DFT calculations. Using two different hybrid PBE0 and B3LYP functionals, combined with the broken symmetry (BS) approach, we found that the BS states of both naphthalene and stilbene complexes have lower energy than the corresponding high-spin (HS) triplet ones. The B3LYP/BS estimated exchange coupling J constants (-16.1 vs. -9.0 cm^{-1} respectively for the naphthalene and stilbene complexes) corroborate well with those obtained previously for other pentavalent diuranium(V) diimide-bridged systems. The computed J value is found to be sensitive to π-network linking the two magnetic U(V) centers. The natural spin density distributions and molecular orbital analyses explain well the antiferromagnetic character of these compounds and clarify the crucial role of the π aromatic spacer in promoting spin polarization and delocalization favoring the magnetic coupling. Furthermore, the effective involvement of the 6*d*/5*f* metal orbitals in metal–ligand bonding plays an important role for the magnetic communication between the two active U(V) 5*f* electrons.

Keywords: diuranium(V) complexes, Magnetic exchange coupling, ZORA/B3LYP, Broken symmetry.

1. Introduction

During the past three decades, the magnetic properties of binuclear actinide complexes attracted attention, at both the experimental and theoretical levels.[1-10] Indeed, their ability to support exotic metal–ligand bonding motifs, large spin–orbit coupling and anisotropy barriers allows potential applications in the field of single-molecule magnets (SMM), as pointed out in several recent reviews.[1-6,11-14] In particular, the unique features of actinide-containing molecules may be exploited for the design and synthesis of new binuclear actinide systems exhibiting magnetic coupling interactions.[15-17] Moreover, the more diffuse *f* orbitals in actinide compared to lanthanide ions[8,18] may lead to stronger magnetic super-exchange.[12] A successful strategy to promote interactions between paramagnetic actinide ions consists of the use of covalently-linked bridging ligands.[5,6,8,19-21]

Despite the growing number of various synthesized actinide-containing complexes, the theoretical study of their magnetic behavior remains a challenge for quantum chemistry.[1,5,6,9,10] If significant progress has been made in the computation of magnetic coupling constants in bridged transition metal systems[22,23] the magnetic properties of actinide complexes were investigated by quantum chemistry methods in only a few studies.[9,10,24,25] Density Functional Theory (DFT) in combination with the hybrid B3LYP functional[26,27] and the Broken-Symmetry (BS) approach,[28,29] was successfully used to explore the electronic structure of actinide-containing molecules and compute their magnetic exchange coupling.[1,19,30-35] Such theoretical approaches could be viewed as useful tools for the design of new actinide bearing compounds with strong magnetic exchange coupling.

The first binuclear magnetic actinide system was reported in the 1990s by Rosen et al.[36] These authors found that the diuranium(V) phenyl-diimide *para*-bridged $[(MeC_5H_4)_3U]_2(\mu\text{-}1,4\text{-}N_2C_6H_4)$ complex shows antiferromagnetic (AF) $5f^1$–$5f^1$ exchange coupling ($J = -19$ cm^{-1}). Afterwards, a growing number of compounds exhibiting unusual U(V)–U(V) couplings have been synthetized, including pentavalent uranium dimers, dioxo-bridged compounds and few examples of diuranium(III), diuranium(IV) and mixed uranium(IV)–transition metal complexes are also known, as recently reviewed (see references herein).[1,11]

Herein, we report a theoretical investigation of two bridged diuranium(V) diimide complexes, i.e. naphthalene-diimide $[(MeC_5H_4)_3U^V]_2(\mu\text{-}1,5\text{-}N_2C_{10}H_6]$ and stilbene-diimide $[(MeC_5H_4)_3U^V]_2(\mu\text{-}1,2\text{-}(4\text{-}NC_6H_4)_2\text{-}C_2H_2]$, for which no extensive and systematic theoretical studies exist. These complexes, exhibiting the $5f^1$-$5f^1$ configuration, were synthetized by Rosen in 1989,[37] but their magnetic properties were not completely clarified by susceptibility measurements and are not yet established. Assuming that nitrogenous ligands promote bridging and electronic communication between paramagnetic actinide centers, a AF coupling character is expected for the bridged-diuranium(V) systems. Two model systems, hereafter called U_2-naphtalene and U_2-stilbene (Scheme 1), are treated, where the MeC_5H_4 ligands of the

actual complexes are replaced by unsubstituted Cp rings. Two possible electron configurations of the two uranium-centered $5f^1$–$5f^1$ electrons were considered for each complex: the f^2–f^2 HS (↑…↑, ferromagnetic), and the f^2–f^2 BS (↑…↓, AF). The corresponding states are schematically represented in Figure 1 for both the U_2-stilbene and U_2-naphthalene diimide complexes. The HS states have spin $S_{max} = S_A + S_B = 1$, with $S_A = S_B = \frac{1}{2}$.

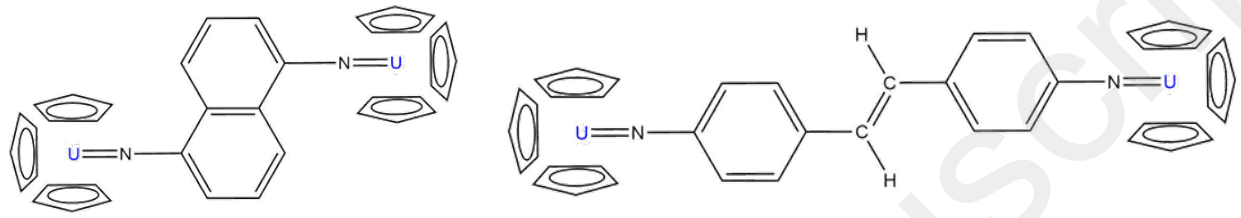

U_2-naphtalene **U_2-stilbene**

Scheme 1: Structure of $[Cp_3U^V]_2(\mu\text{-L})$ (L = stilbene- and naphthalene-diimide) complexes. They are denoted as U_2-naphtalene and U_2-stilbene.

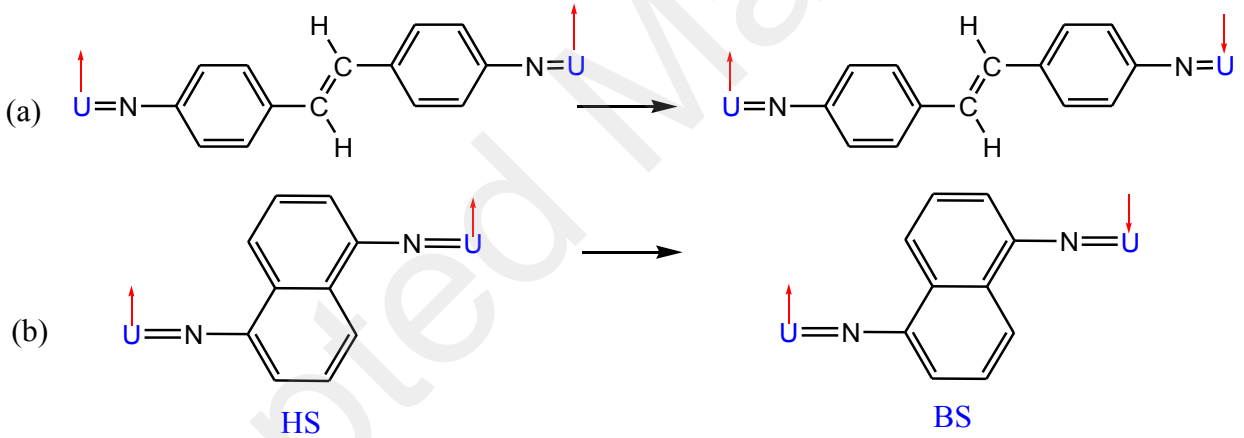

Figure 1: Schematic presentation of the ferro- and antiferro-magnetic couplings for (a) stilbene- and (b) naphthalene-diimide. The Cp ligands are omitted for clarity.

By studying such systems, using DFT computations coupled to the BS recipe, we aim at assessing the nature and strength of the exchange coupling by drawing magneto-structural correlations between the two models $[Cp_3U^V]_2(\mu\text{-L})$ (L = stilbene- and naphthalene-diimide). In particular, the roles of the aromatic spacer, the co-ligand Cp and uranium(V) 5*f* orbitals will be investigated. Prior to this work, the same DFT/BS methodology has been successfully applied by some of us[32–35] and by others[19,30,31] to investigate the magnetic exchange interactions in such systems. This work aims to provide an in-depth understanding, at the molecular level, of the magnetic properties of these two diuranium model

compounds, and may be helpful for the design and performance improvement of f-element single-molecule magnets.[14-20]

2. Computational details

All calculations were performed with the Amsterdam Density Functional (ADF) program (ADF2019.302 release).[38,39] Relativistic corrections, obviously important for U-containing compounds, have been introduced via the zeroth order regular approximation (ZORA)[40,41] accounting for scalar relativistic effects. Molecular structure drawings, spin densities and molecular orbital plots were generated using the ADF-GUI auxiliary program.[39] Finally, in these calculations the ADF integration accuracy parameter was set to 8.0.

a. Geometry optimizations

We started our investigations by optimizing the equilibrium structures of U_2-naphtalene and U_2-stilbene. These computations were done using the exchange and correlation functionals of Becke and Perdew (BP86),[42−44] combined with the triple-ζ-plus polarization (TZP) Slater type orbital (STO) basis sets. We adopted a spin-unrestricted formalism. Thus, at this level of theory, we performed all geometry optimizations followed by analytical computations of the harmonic vibrational frequencies, to ensure that the optimized structures correspond to local minima on the potential energy surface (all real frequencies).

The geometrical parameters of $[(MeC_5H_4)_3U^V]_2(\mu\text{-}1,5\text{-}N_2C_{10}H_6]$ and $[(MeC_5H_4)_3U^V]_2(\mu\text{-}1,2\text{-}(4\text{-}NC_6H_4)_2\text{-}C_2H_2]$ derived by Rosen[37] were used as an initial guess for the subsequent full geometry optimizations of the U_2-naphtalene and U_2-stilbene model complexes. In the BP86 calculations, the frozen-core approximation, where the core density is obtained from four-component Dirac–Slater calculations, has been applied to all atoms, i.e. the 1*s* core electrons of carbon and nitrogen were kept frozen. For the actinide, the small frozen-core U[5*d*] was used, resulting in a valence space composed of the 5*f*/6*s*/6*p*/6*d*/7*s*/7*p* shells (14 valence electrons). Such methodology, whose validity has been proven in previous theoretical works,[25,32-35,45,46] is able reproducing the experimental geometries of *f*-element compounds with good accuracy.

Furthermore, we carried out single-point calculations to estimate the exchange coupling constant J using the two B3LYP[47,48] and PBE0[49] hybrid functionals. Spin-orbit (s-o) corrections to the energy have not been considered, although they are relevant for pure spin states and their effect is noticeable when computing properties like electron affinities of actinide complexes.[50] Nevertheless, they could introduce spurious contributions when computed for the fictitious BS state. The procedure we adopted in this study is in line with previous DFT calculations of magnetic exchange coupling for diuranium(IV) and (V) species,[19,20,30-33] which did not include spin-orbit corrections either.

b. Evaluation of the exchange coupling

The magnetic interaction between two atomic spins is usually described by the Heisenberg-Dirac-Van Vleck (HDvV) Hamiltonian, given by $\hat{H} = -2 J \hat{S}_A \cdot \hat{S}_B$, where J is the coupling constant between the A and B magnetic sites with total spin operators $\hat{S}_A$ and $\hat{S}_B$. A positive sign of the coupling constant J indicates a ferromagnetic interaction (parallel alignment of spins), whereas the negative sign indicates an antiferromagnetic interaction (anti parallel alignment of spins). It is noteworthy that accurate quantum mechanical evaluation of the coupling constant requires multideterminantal post-Hartree–Fock calculations.[9,10,22,23] However, such ab initio methodologies are computationally challenging for large molecular systems containing actinides. A good alternative is provided by the combined DFT/BS approach,[28,29] where the exchange coupling constant J can be extracted from the difference of the high spin (HS) and the BS state energies ($\Delta E = \boldsymbol{E_{BS}} - \boldsymbol{E_{HS}}$). For both the U_2-stilbene and U_2-naphthalene diimide complexes, the BS state energy has been obtained by performing a single point SCF calculation using the molecular orbitals (MOs) of the HS structure as starting guess, and changing the spin on the second uranium atom (using the spin-flip recipe available in the ADF program).[51] Moreover, we must keep in mind that in the evaluation of the coupling constant J, energy differences are often smaller than ~0.5 kcal/mol (i.e. ≈175 cm^{-1}).[52] Anyway, the DFT/BS approach based on the hybrid functional B3LYP turns out to be reliable for an accurate prediction of the coupling constant J, not only in binuclear transition metal complexes,[22,23,53] but also in actinide-containing molecules,[19,30-35] even though the use of the DFT monodeterminantal approach in such cases is a subject of debate.[9,19,54]

Yamaguchi et al.[55] have suggested an expression for the correct evaluation of J within the BS approach, which should be valid over the full range of coupling strengths, from the weak to the strong overlapping limit. The corresponding expression is:

$$\boldsymbol{J} = \frac{\boldsymbol{E_{BS}} - \boldsymbol{E_{HS}}}{< \boldsymbol{S^2} >_{\boldsymbol{HS}} - < \boldsymbol{S^2} >_{\boldsymbol{BS}}}$$

where $< \boldsymbol{S^2} >_{\boldsymbol{HS}}$ and $< \boldsymbol{S^2} >_{\boldsymbol{BS}}$ are the HS and BS mean values of the squared spin $\boldsymbol{S}$ operator, respectively.

The reliability of the BS approach using Yamaguchi's formula has been discussed earlier and validated,[19,30-35,56,57] where it was shown that computations of the magnetic coupling constants at the B3LYP level generally lead to satisfactory results and good agreement with both high-level post-HF computations and experimental findings.[1]

3. Results and Discussion

a. Equilibrium structures

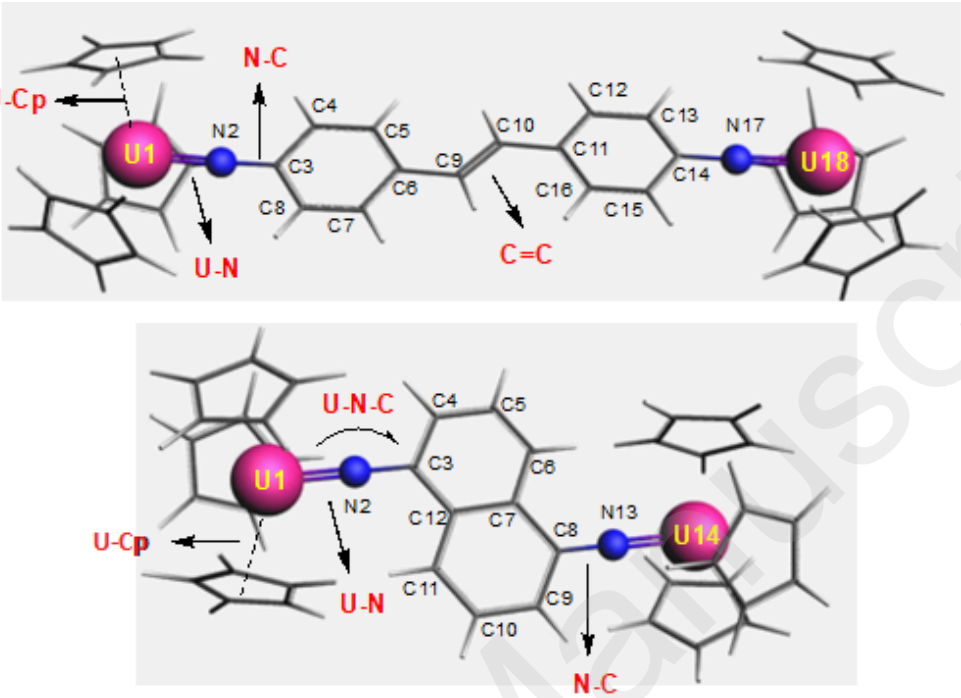

Figure 2: Optimized molecular structures of U_2-stilbene (top) and U_2-naphtalene (bottom) model complexes. We give also the atom numbering and the main geometrical parameters (in red) listed in Table 1.

Table 1: Relevant average ZORA/BP86 optimized bonds distances (Å) and angles (°) for $[Cp_3U^V]_2(\mu$-L) (L = stilbene- and naphthalene-diimide) model complexes in their triplet HS state. See Figure 2 for the definition of the geometrical parameters.

Geometrical parameter	U–N	N–C	U–Cp [f]	C=C	U–N–C	U–U
U_2–naphtalene [a]	1.973	1.368	2.596	1.438	168.9	10.112
$[(MeCp)_3U^V]_2(\mu$-1,5-N_2 naphtalene] [b]	2.00	1.40	-	-	-	9.9
U_2–stilbene [a]	1.984	1.369	2.508	1.359	175.9	16.220
$[(MeCp)_3U^V]_2(\mu$-1,5-N_2 stilbene] [b]	2.00	1.40	-	1.30	-	16.0
$[(Cp)_3U^V]_2(\mu$-1,4-$N_2C_6H_4)$ [c]	2.084	1.442	2.59	-	176.5	10.103
$(MeCp)_2U[=$N-2,4,6-$^tBu_3$-$C_6H_2]$ [d]	1.965(8)	1.415(11)	2.505	-	171.0(7)	-
$[(MeCp)_3U(=NC_6H_5)]$ [e]	2.019(6)	1.36(1)	2.48	-	167.4(6)	-

[a] This work, [b] Ref [37], [c] Ref [32], [d] Ref [58], [e] Ref [59], [f] Cp (C_5H_5) centroid.

Since no X-ray experimental structures are available for the complexes under consideration, the molecular parameters of Rosen[37] were used as an initial guess for the geometry optimizations of both U_2-naphtalene and U_2-stilbene, i.e. bond lengths U(V)–N ≈ 2.00 Å, N–C ≈ 1.40 Å, C=C ≈ 1.30 Å, and metal–metal distance U(V)–U(V) ≈ 9.9 *vs*. 16.0 Å for U_2-naphtalene and U_2-stilbene, respectively. The molecular structures obtained from the ZORA/BP86 geometry optimizations of the two U_2-naphtalene and U_2-stilbene models are displayed in Figure 2, together with the definition of a few selected geometrical parameters. In the Supplementary Material, we give the full set of the optimized Cartesian coordinates of the U_2-naphtalene and U_2-stilbene complexes (Tables S1 and S2) and their IR simulated spectra (Figures S1 and S2).

In Table 1, we report optimized bond distances and angles for the HS state of the two model complexes. Compared to the model values of Rosen, we obtain slightly longer U(V)–U(V) and U(V)–N distances and a slightly shorter (N–C) distance for both complexes. Since the differences are small, we conclude that our theoretical data are in good agreement with the experimental ones. Table 1 shows also that the U–Cp distance is longer in U_2-naphtalene than in U_2-stilbene. Most likely, this difference is due to the steric hindrance between the Cp rings and the bridging ligand in the former complex. This is connected also with the smaller U-N-C angle (of ≈169°) computed for U_2-naphtalene compared to that of U_2-stilbene (of ≈176°). However, these angles remain close to 180°, ensuring favorable molecular orbital overlap between the U, N moieties and naphthalene/stilbene (see below). One can note the dihedral angle U-N-C-C involving naphthalene and stilbene carbon atoms equal to 0.0° insuring the well planarity for the systems.

For comparison, we give also in Table 1 the DFT structural parameters for the para-imido diuranium ($5f^1$-$5f^1$) $[(Cp)_3U^V]_2(\mu\text{-}1,4\text{-}N_2C_6H_4)$ complex[36] and X-ray data for the $(MeCp)_2U[=N\text{-}2,4,6\text{-}{}^tBu_3\text{-}C_6H_2]$ and $[(MeCp)_3U(=NC_6H_5)]$ monomer complexes, as determined by Graves et al.,[58] Brennan and Andersen,[59] respectively. In overall, the DFT calculations for the model systems in Table 1 correlate well with experimentally determined metrical parameters for similar systems. In particular, the U–N bond distances of 1.973 Å and 1.984 Å for U_2-naphtalene and U_2-stilbene, respectively, are within the typical range of multiple uranium(V)-imide bonds.[58-60] Furthermore, the linear U–N–C coordination geometry, particularly in U_2-stilbene (*ca*. 176°), is indicative of multiple bonding. Such coordination throughout the π-bridging ligand was also found in phenylene-diimide diuranium(V) species, and was attributed to a significant participation of the uranium 5*f* orbitals in metal–N bonding.[1,5,6,30,32,33,36] These orbitals will also maximize the possibility of electronic and magnetic communication between the two U(V) metal centers through the π-bridging ligand, which could favor magnetic super-exchange.[1,8,11-14,19,20] Note that the

computed U(V)–U(V) distance of *ca.* 10.1 Å for U_2-naphtalene compares well with that of 10.103 Å reported for the AF para-phenylene-diimide diuranium(V) complex.[32,36]

b. Electronic structure analysis

In order to investigate the electronic structure and the nature of the metal-ligand bonding, natural population analysis (NPA)[61] as well as Mayer[62] and Nalewajski-Mrozek (NM)[63,64] bond order analysis were performed on U_2-naphthalene and U_2-stilbene, at their optimized equilibrium geometries, with the ZORA/B3LYP/TZP approach. The NPA method is a better alternative to Mulliken population analysis[65] (MPA) for probing the covalence in f-element complexes, leading to results in better agreement with the experimental trends.[66] For bonded nitrogen and uranium atoms, natural atomic net charges (q), as well as Mayer and Nalewajski-Mrozek (NM) bond orders are reported in Table 2.

Table 2: ZORA/B3LYB NPA of atomic net charges (q in C), Mayer and NM average U–N, N–C and C=C bond orders of the U_2-stilbene and U_2-naphthalene complexes in their HS/BS states. See Figure 2 for the definition of the distances.

models	NPA (q)		U–N		N–C		C=C	
	U	N	Mayer	NM	Mayer	NM	Mayer	NM
U_2–naphtalene								
HS	0.74	-0.55	1.791	2.701	1.140	1.278	1.306	1.295
BS	0.74	-0.55	1.784	2.715	1.143	1.251	1.304	1.292
	U_2–stilbene							
HS	0.73	-0.53	1.807	2.688	1.129	1.292	1.637	1.739
BS	0.73	-0.53	1.796	2.697	1.134	1.264	1.629	1.729

The NPA charges on the uranium atoms are calculated to be +0.74 *e* in U_2-naphtalene and +0.73 *e* in U_2-stilbene, *i.e.* much smaller than the formal value of +5 *e* in pentavalent uranium. This is indicative of the relatively strong covalent character of the metal–ligand bonding in these compounds, due to extensive ligand-to-metal charge donation. These covalent contributions originate mainly from the favorable energy matching between the d/f orbitals of the metal and those of the ligands.[25,67,68] This is not only important for the π-network bridging ligand in U_2-naphthalene and U_2-stilbene, but could also favor super-exchange coupling interactions.[1,5,6,11,32,33] The Mayer and NM bond orders in Table 2 further attest the covalent nature of the U–N bonds in these complexes and their multiple bond character. Indeed, we calculate Mayer and NM bond orders of 1.791 and 2.701, respectively, for U_2-naphthalene, and 1.807 and

2.688, respectively, for U_2-stilbene, when both species are considered in their HS state. As stated previously,[1,5,6,11-14] the multiple bonds between uranium and nitrogen atoms, together with the strong π ligand-to-metal donation, will lead to significant electronic communication which may favor metal–metal super-exchange coupling. The calculated bond orders for the N–C and C=C bonds in Table 2 are consistent with the delocalization of the π electron system in these complexes.

c. Molecular Orbital Analysis

In order to study the π-network pathway that enables electronic communication between the two U(V) spin centers, we performed a MO analysis using B3LYP. The frontier MO diagrams of the U_2-naphthalene and U_2-stilbene diimide models in their HS/BS states are depicted in Figures 4 and 5. In these diagrams the notation (6*d*/5*f*/U/ligand)% represents, respectively, the percent weight of the contributions to a given MO from the 6*d*, 5*f* orbitals of the metals, from all the atomic orbitals of the metals and from those of the ligands.

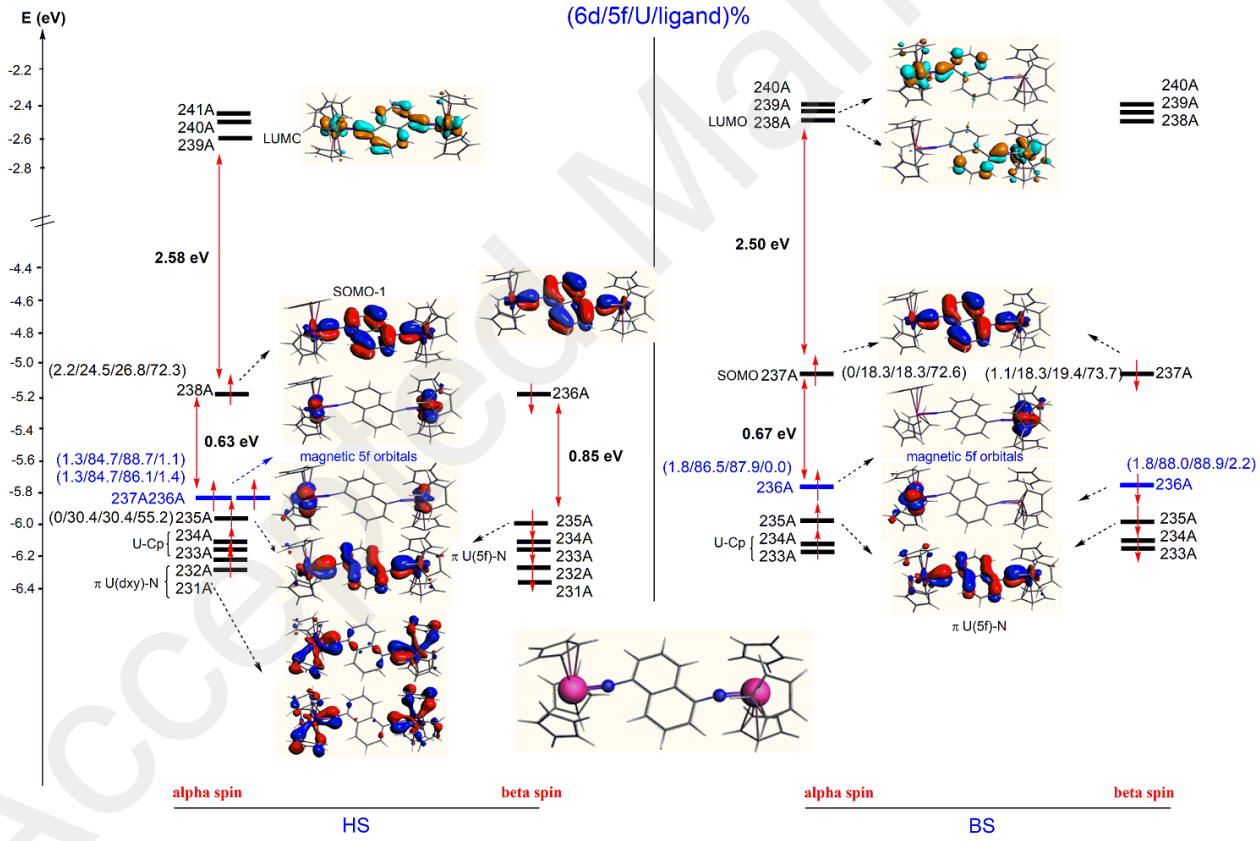

Figure 3: B3LYP Frontier MO diagram of the U_2-naphtalene in its HS/BS states. The occupied MOs are in blue and red and the virtual ones are in cyan and brown.

As shown in the left panel of Figure 3, the highest occupied MO (HOMO) of U_2-naphtalene in its HS (triplet) state is not composed of pure 5*f* orbitals. This orbital is entirely delocalized over the two metals and the linking bridge. The α and β spin-orbital components of the HOMO (α-238A and β-236A) are not rigorously degenerate because of the spin-unrestricted DFT formalism. This MO exhibits large π-bonding interactions, involving uranium 5*f* orbitals and those of the covalently bridging ligand, as shown by the percent weight contributions. The two degenerate α-237A and α-236A spin-orbitals, 0.63 eV lower in energy, are composed essentially of the 5*f* orbitals of the two metals, with practically no contributions from the bridging ligand orbitals. It is noteworthy that the corresponding singly occupied MOs (SOMOs), bearing the two $5f^1$-$5f^1$ active spin electrons that are responsible for the magnetic properties of the molecule, are delocalized on the two U(V) spin centres. The delocalization of the lower-energy orbital 235A contributes to the bridging ligand ability to enhance the metal–metal super-exchange interaction. Similarly, for the BS state (Figure 3, right panel), the HOMO is composed of the α-237A and β-237A occupied spin-orbitals responsible for the metal–ligand π-bonding, while the two SOMOs, 0.67 eV lower in energy, are mainly composed of the uranium 5*f* orbitals and are localized on the two U(V) spin centres. In the BS state, the two magnetic 5*f* SOMOs are completely localized on each of the two U(V) spin centers. Most notably, the calculated 5*f* splitting is larger in the BS state than in the HS one, indicating a greater involvement of the 5*f* orbitals in bonding in favor of more metal–ligand–metal electronic π-delocalization.[32,33,69]

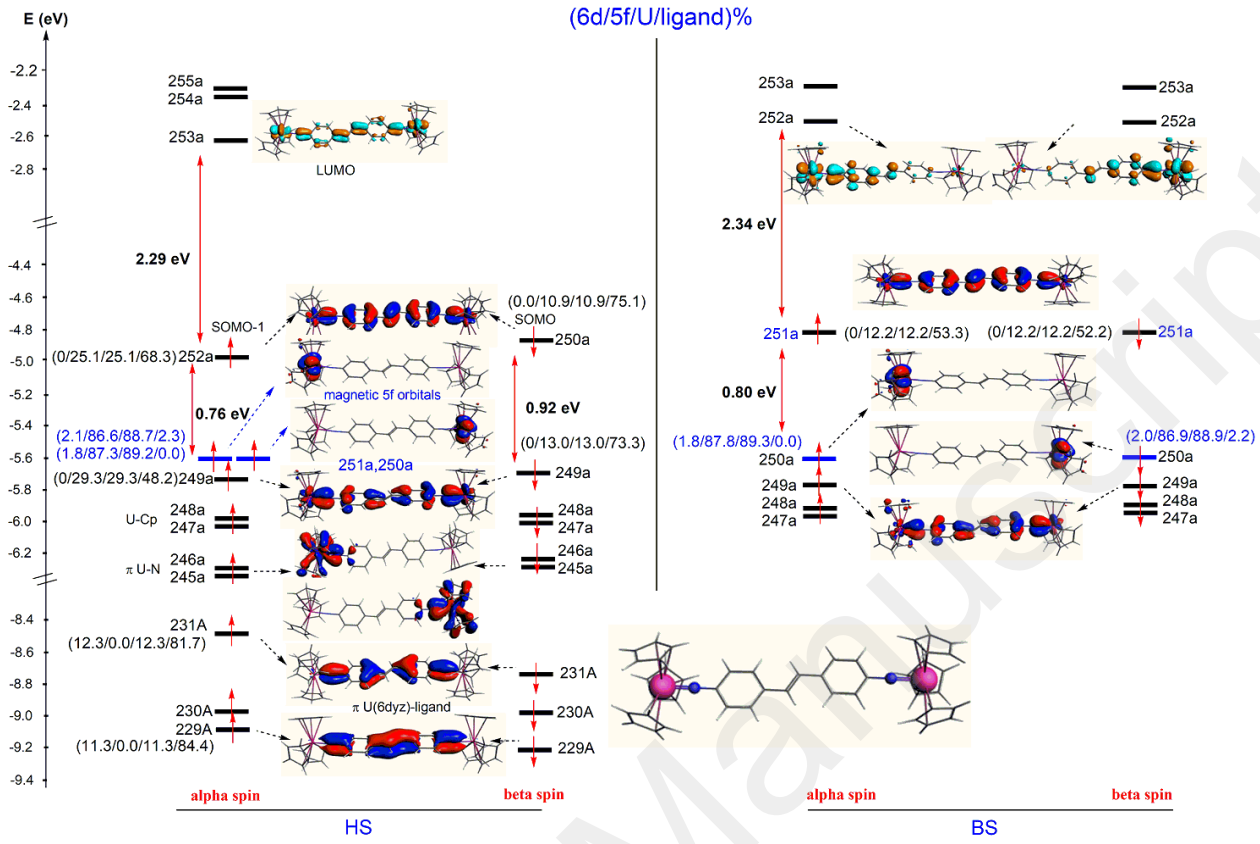

Figure 4: B3LYP Frontier MO diagram of the U_2-stilbene in its HS/BS states. The occupied MOs are in blue and red and the virtual ones are in cyan and brown.

For the U_2-stilbene, the HS/BS diagrams depicted on Figure 4 exhibit a close resemblance to the U_2-naphtalene case. For U_2-stilbene in both the HS and BS states, the SOMOs bearing the two $5f^1$–$5f^1$ active spin electrons are separately localized on the two metal U(V) spin centers. With respect to the HOMO energy, the two degenerate SOMOs are more stabilized in the BS (0.80 eV) than in the HS (0.76 eV) state. The factors that lead to an AF coupling, namely the electronic factors favoring communication between the two magnetic centres, already appear in the MO analysis.

d. Magnetic properties

i) Evaluation of the exchange coupling constant J

Following the MO analysis, we study now the U(V)–U(V) magnetic coupling in the two complexes. Unfortunately, the magnetic character of these systems has not yet been clearly established by variable temperature measurements.[37] Here, the evaluation of the magnetic coupling constant will be done using the DFT/BS approach[28,29] as detailed above. The two complexes under study exhibit similar $5f^1$-$5f^1$ electron configurations, molecular orbitals and energy level patterns.

In Table 3, we report the computed total bonding energy (TBE), energy differences (ΔE), mean value of the squared spin operator ($\langle S^2 \rangle$) for the estimation of the spin contamination, as well as the computed exchange coupling constants J using the spin-projected Yamaguchi's formula (*vide supra*).

Table 3: Computed B3LYP TBE for the HS (TBE_{HS}) and BS (TBE_{BS}) states (in eV), $\Delta E = E_{BS} - E_{HS}$, in cm^{-1}) energy differences, $\langle S^2 \rangle_{HS/BS}$ values, and exchange coupling J (in cm^{-1}) constant for the U_2-naphthalene and U_2-stilbene diimide complexes.

Complex	TBE_{HS}	TBE_{BS}	ΔE	$\langle S^2 \rangle_{HS}$	$\langle S^2 \rangle_{BS}$	J
U_2-naphtalene	-591.8901	-591.8920	-15.48	2.14	1.18	-16.1
U_2-Stilbene	-647.5112	-647.5122	-8.68	2.17	1.23	-9.0

For the triplet $5f^1$-$5f^1$ HS state systems, Table 3 shows that $\langle S^2 \rangle_{HS}$ exhibit correct values (≈ 2), indicating that almost no spin contamination occurs. Furthermore, as expected, the computed $\langle S^2 \rangle_{BS}$ values are intermediate between those of a singlet ($\langle S^2 \rangle = 0$) and triplet ($\langle S^2 \rangle = 2$) states. For both systems, the BS energy is computed slightly, but significantly, lower than the HS one, indicating, as expected, an AF character of the U(V)–U(V) exchange coupling interaction. As shown in Table 3, the computed J values for U_2-naphtalene (–16.13 cm^{-1}) and U_2-stilbene (–9.04 cm^{-1}) are distinctly different, but compare rather well with those, ranging from –12 to –19 cm^{-1}, reported in the literature for diimide diuranium(V) species.[1,5,30,32,36]

We found that the PBE0 hybrid functional compared to B3LYP, gives a much higher HS/BS energy differences than what is expected for magnetic binuclear actinide diimide systems.[1,11,30-33,36,69] Consequently, the PBE0 computations lead to too high values of the coupling, i.e. -77.2 and -59.6 cm^{-1} for U_2-naphthalene and U_2-stilbene, respectively. Among the two functionals, B3LYP/BS appears to be the best technique for modelling actinide-containing molecules with magnetic super-exchange interactions.

As previously reported in the literature,[1,5,6,11-14] geometrical and electronic effects on the exchange coupling constant are comparable. Notably, it has been found that in several diuranium(V) systems with long metal–metal distances (>10 Å), conjugation across the π-bridging ligand is likely to promote electronic communication, leading to AF super-exchange coupling.[1,19,32,33,36,69,70] Therefore, the magnitude of the magnetic exchange in U_2-naphthalene and U_2-stilbene will result from two opposite effects: (i) the large values of the metal-metal distances (Table 1), which should induce small values of J, and (ii) electron delocalization effects, which should lead to large J values.[37]

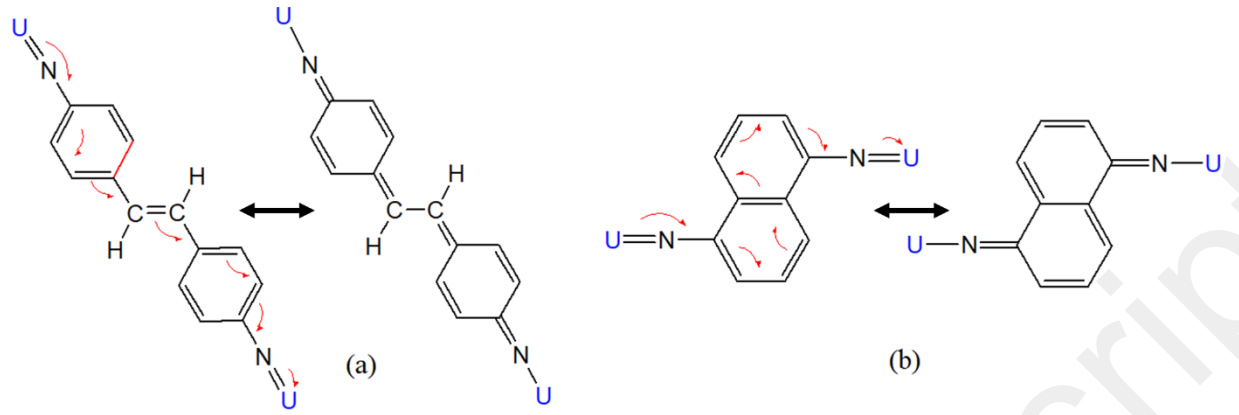

Figure 5: Resonance structures of the (a) U_2-stilbene and (b) U_2-naphthalene complexes. The Cp groups were omitted for simplicity.

Since electron delocalization effects should be similar in U_2-naphthalene and U_2-stilbene (Figure 5), the difference in exchange coupling strength is most likely due to the U–U distance, which is larger in the latter complex (Table 1). In particular, the U(V)–U(V) distance in U_2-stilbene is calculated to be ≈16.2 Å which is longer than in other similar bridged-diimide compounds.[1] This is in line with the available data on other diimide compounds. Let's cite, for instance, the work of Newell et al.[19] dealing with the *para*-diethynylbenzene diuranium(IV) $[(NN_3)_2U_2(p\text{-DEB})]$ $(NN'_3=[N(CH_2CH_2NSi^tBuMe_2)_3]$ complex. These authors reported a rather long metal-metal distance of 12.9499(1) Å observed by X-ray spectroscopy, and calculated a weak $5f^2$–$5f^2$ antiferromagnetic coupling of –0.1 cm^{-1}. In addition, Kiplinger and co-workers[69] pointed out a significant electronic communication between phenylene-diketimide-linked U(IV) centers, separated by 10.956 Å and exhibiting a $5f^2$–$5f^2$ configuration. For the same system, at the DFT/B3LYP level, Meskaldji et al.[33] calculated a metal-metal distance of 11.057 Å and a weak antiferromagnetic exchange coupling ($|J| < 5$ cm^{-1}). More interestingly, another dinuclear U(V)–U(V) complex reported by Walensky and co-workers,[70] where the two paramagnetic U(V) centres linked by the *para*-benzoquinone exhibit a weak AF coupling ($J = -0.6$ cm^{-1}). These findings are also valid for oxo-bridged complexes,[34,35] for which some of us revealed that the magnetic exchange coupling is more sensitive to changes in the U−U distance and UOU angles at core geometry than to modifications in the coordination environment around the magnetic core. Conversely, for the $[\{U(N^tBu)_2(I)_2(bpy)\}_2]$ model system, Spencer et al.[30] calculated at the DFT/BS level a coupling constant J of –12 cm^{-1}, smaller than in other *para*-bis(imido) diuranium(V) systems with larger U(V)–U(V) distances.[32] In such cases the electronic nature of the bridge, rather than the distance between the metal atoms, determines whether AF exchange occurs.

ii) Spin densities

To gain a deeper insight into the magnetic character of the U_2-naphtalene and U_2-stilbene systems and explain their different exchange coupling strengths, spin density analyses have been carried out for the HS and BS states. The exchange coupling between the magnetic centers, can be explained by the spin polarization and spin delocalization phenomena, as described earlier by Kahn.[71] For U_2-naphtalene and U_2-stilbene, the obtained spin density distributions (difference between the α and β electron densities) along the path linking the two magnetic U(V) metal centres are displayed in Figure 6. Furthermore, both NPA and MDC (multipole derived charges) analysis[72] of the atomic spin populations as reported in Table 4, lead to equivalent results, although NPA gives a metal spin population greater than 1 in absolute value compared to the MDC analysis result.

As shown in Figure 6, the spin density in the HS state is mainly localized on the two uranium(V) and nitrogen centers, with a small density spread along the path linking the two metals and significant depletion at the C7=C12 and C9=C10 bonds of U_2-naphtalene and U_2-stilbene, respectively. In the BS states of both systems, the two magnetic U(V) centres are AF coupled, with significant spin density contributions from the bridged ligand atoms, and no major depletions. The involvement of spin polarization and spin delocalization in the mechanism driving the AF coupling in U_2-naphtalene and U_2-stilbene emerges clearly through the latter (BS) spin density distribution. We also note that the Cp ligands are practically not involved in this coupling and, thus, are not expected to play a significant role. This justifies *a posteriori* the use of Cp instead of MeCp for the present modelling of the uranium compounds synthetized by Rosen.[37]

U_2-naphtalene

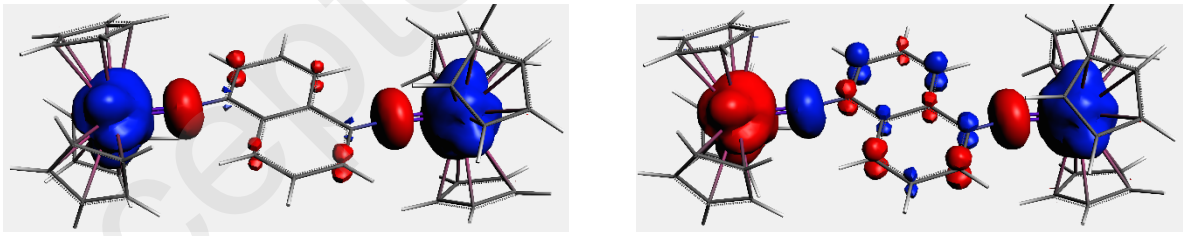

U_2-stilbene

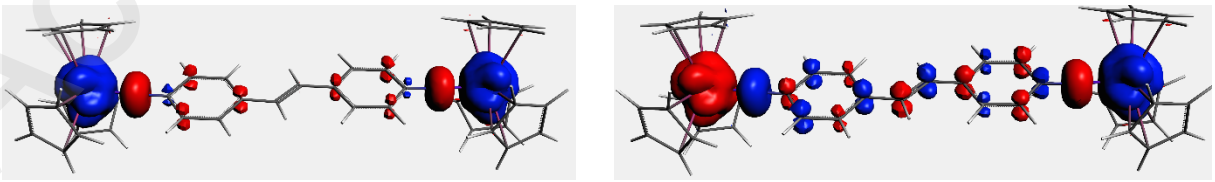

HS **BS**

Figure 6: Spin density plots for the HS triplet and BS states of U_2-naphtalene (Top) and U_2-stilbene (Bottom) (blue/red color: positive/negative spin density). The isodensity surface corresponds to a value of 0.0025 e $bohr^{-3}$.

Table 4: ZORA/B3LYP/NPA and MDC computed atomic natural spin populations of U_2-naphtalene and U_2-stilbene diimide model complexes in their HS and BS states as numbered on the Figure 2.

U_2-naphtalene					U_2-Stilbene				
	NPA		MDC			NPA		MDC	
Atom	HS	BS	HS	BS	Atom	HS	BS	HS	BS
U1	1.370	-1.400	0.969	-0.989	U1	1.392	-1.434	0.993	-1.022
N2	-0.197	0.209	-0.100	0.106	N2	-0.214	0.219	-0.111	0.113
C3	0.028	-0.053	0.012	-0.029	C3	0.030	-0.055	0.014	-0.033
C4	-0.045	0.069	-0.040	0.063	C4	-0.040	0.055	-0.036	0.049
C5	0.007	-0.036	0.004	-0.033	C5	0.013	-0.035	0.010	-0.031
C6	-0.034	0.062	-0.034	0.061	C6	-0.033	0.055	-0.030	0.046
C7	-0.012	-0.040	-0.018	0.047	C7	0.014	-0.036	0.011	-0.031
C8	0.028	0.053	0.012	0.029	C8	-0.037	0.055	-0.033	0.045
C9	-0.045	-0.069	-0.007	-0.063	C9	-0.011	-0.033	-0.007	-0.026
C10	0.007	0.036	0.004	0.033	C10	-0.010	0.032	-0.007	0.027
C11	-0.034	-0.062	-0.034	-0.061	C11	-0.037	-0.058	-0.033	-0.049
C12	-0.012	0.040	-0.014	-0.048	C12	0.016	0.037	0.013	0.032
N13	-0.197	-0.209	-0.100	-0.106	C13	-0.040	-0.053	-0.036	-0.047
U14	1.370	1.400	0.969	0.989	C14	0.034	0.057	0.016	0.034
					C15	-0.044	-0.059	-0.041	-0.053
					C16	0.016	0.037	0.013	0.033
					N17	-0.212	-0.220	-0.106	-0.118
					U18	1.394	1.431	1.003	1.031

From data in Table 4, we note that the HS states of both systems exhibit quasi-localized spin densities on the two magnetic uranium(V) centers, with non-negligible values on the neighboring nitrogen atoms and only slight delocalization within the bridging naphthalene and stilbene ligands. Table 4 shows a higher accumulation of spin density between the two magnetic centers, when passing from the HS to BS states. Moreover, the U_2-naphtalene natural spin densities (NPA) on the uranium atoms are 1.370 in the

HS state, while they become -1.400 and 1.400 in the BS state. A similar trend is observed for the U_2-stilbene. Notably, the remarkable sign alternation of the BS spin densities along the path linking the two magnetic centers, due to spin polarization, proves the AF exchange coupling. As it can be seen in Figure 6, the atoms C7 and C12 in U_2-naphtalene and C9 and C10 in U_2-stilbene exhibit almost vanishing spin populations in the HS states, while in the BS states the corresponding spin densities are increased by spin-delocalization. This trend seems to be more pronounced in U_2-naphtalene than in U_2-stilbene, and is likely to explain the difference in exchange coupling strength (Table 3).

4. Conclusions

The magnetic exchange coupling interactions in diuranium(V) diimide L-bridged complexes $[Cp_3U^V]_2(\mu\text{-L})$ (L = stilbene and Naphthalene), exhibiting a $5f^1$-$5f^1$ electron configuration, have been investigated for the first time using relativistic ZORA/DFT computations combined with the B3LYP and PBE0 hybrid functionals and the broken symmetry (BS) methodology. The used theoretical approach was successful in predicting the antiferromagnetic (AF) character of the two uranium complexes, in agreement with the literature. B3LYP results appear to be more reliable than the PBE0 ones. Furthermore, the super-exchange coupling has been rationalized according to the natural spin density distributions, revealing the crucial role of spin polarization and spin delocalization in AF interactions. Such interactions in the studied systems are mediated by the aromatic diimide bridges, and are mainly due to the effective π-overlap between the *5f* orbitals of the metals and nitrogen atomic orbitals, where the resulting MOs are spread along the path linking the two magnetic uranium(V) centers. The analysis of the Mayer and Nalewajski-Mrozek (NM) bond orders reveals the multiple bond character of the U-N bonds. The covalence effects and the strong π ligand-to-metal donation favor electronic communication and metal–metal super-exchange coupling. Finally, the good performance of the ZORA/B3LYP/BS procedure is remarkable. Through this approach, valuable information can be extracted on the bridging ligands and used to develop other uranium(V) compounds displaying unprecedented magnetic super-exchange coupling.

Acknowledgments

We acknowledge the Algerian PRFU project (2018-2022: Grant No. B00L01UN250120180015) and the French GENCI IDRIS and GENCI-CINES for an allocation of computing time (Grant No. 2018-2019-080649).

References

1. Belkhiri L, Le Guennic B, Boucekkine A (2019) DFT Investigations of the Magnetic Properties of Actinide Complexes. Magnetochemistry. 5:15. DOI:10.3390/magnetochemistry5010015
2. Feng M, Tong M-L. (2018) Single Ion Magnets from 3d to 5f: Developments and Strategies. *Chem. Eur. J.* 24:7574–7594. DOI :10.1002/chem.201705761
3. Liddle ST, van Slageren, Layfield R, A Murugesu, M Eds (2015) Lanthanides and Actinides in Molecular Magnetism. J Wiley VCH/ Weinheim 315–340. DOI :10.1002/anie.201509764
4. Magnani N. (2014) Spectroscopic and magnetic investigations of actinide-based nanomagnets. Int J Quantum Chem. 114: 755–759. DOI : 10.1002/qua.24656
5. Rinehart JD, Harris TD, Kozimor SA, Bartlett BM, Long JR (2009) Magnetic Exchange Coupling in Actinide-Containing Molecules. Inorg Chem 48: 3382−3395. DOI: 10.1021/ic801303w
6. Lukens WW, MD Walter (2010) Quantifying Exchange Coupling in f-Ion Pairs Using the Diamagnetic Substitution Method. Inorg Chem 49: 4458−4465. DOI: 10.1021/ic100120d
7. Boucekkine A, Belkhiri L (2013) f-Element Complexes. In: Jan Reedijk and Kenneth Poeppelmeier, Editors. Comprehensive Inorganic Chemistry II. Oxford: Elsevier 9: 277-319. DOI: 10.1016/B978-0-08-097774-4.00910-4.
8. Tatebe CJ, Kiernicki JJ, Higgins RF, Ward RJ, Natoli SN, Langford JC, Christopher LClark, Matthias Zeller, Paul Wenthold, Matthew PShores, Justin RWalensky, Suzanne CBart (2019) Investigation of the Electronic Structure of Aryl-Bridged Dinuclear U(III) and U(IV) Compounds. Organometallics 38(5): 1031-1040. https://doi.org/10.1021/acs.organomet.8b00794
9. Spivak M, Vogiatzis KD, Cramer CJ, de Graaf C, Gagliardi L (2017) Quantum Chemical Characterization of Single Molecule Magnets Based on Uranium. J Phys Chem A 121: 1726–1733. DOI : 10.1021/acs.jpca.6b10933
10. Gaggioli CA, Gagliardi L (2018) Theoretical Investigation of Plutonium-Based Single-Molecule Magnets. Inorg Chem 57: 8098–8105. DOI: 10.1021/acs.inorgchem.8b00170.
11. Gardner BM, King DM, Tuna F, Wooles AJ, Chilton NF, Liddle ST (2017) Assessing Crystal Field and Magnetic Interactions in Diuranium UIV–E–UIV cores (E = S, Se, Te). Chem Sci 8: 6207–6217. DOI:10.1039/C7SC01998J
12. Liddle ST, van Slageren J (2015) Improving f-element single molecule magnets. Chem Soc Rev 44: 6655−6668. DOI: 10.1039/c5cs00222b
13. Rinehart JD, Long JR (2011) Exploiting Single-Ion Anisotropy in the Design of f-Element Single-Molecule Magnets. Chem Sci 2: 2078−2085. DOI**:** 10.1039/C1SC00513H
14. Meihaus KR, Long JR (2015) Actinide-Based Single-Molecule Magnets. Dalton Trans Int Ed 44: 2517−2528. DOI: 10.1039/c4dt02391a

15. McAdams SG, Ariciu AM, Kostopoulos AK, Walsh JPS, Tuna F (2017) Molecular single-ion magnets based on lanthanides and actinides: Design considerations and new advances in the context of quantum technologies. Coord Chem Rev 346: 216–239. DOI: 10.1016/j.ccr.2017.03.015
16. Magnani N, Caciuffo R (2018) Future Directions for Transuranic Single Molecule Magnets. Inorganics 6: 26. DOI: 10.3390/inorganics6010026
17. Pedersen KS, Dreiser J, Weihe H, Sibille R, Johannesen HV, Sorensen MA, Nielsen BE, Sigrist M, Mutka H, Rols S, Bendix J, Piligkos S (2015) Design of Single-Molecule Magnets: Insufficiency of the Anisotropy Barrier as the Sole Criterion. Inorg Chem 54: 7600−7606. DOI: 10.1021/acs.inorgchem.5b01209
18. Neidig ML, Clark DL, Martin RL (2013) Covalency in f-element complexes. Coord Chem Rev 257: 394–406. DOI: 10.1016/j.ccr.2012.04.029
19. Newell BS, Rapp AK, Shores MP (2010) Experimental Evidence for Magnetic Exchange in Di- and Trinuclear Uranium(IV) Ethynylbenzene Complexes. Inorg Chem 49: 1595–1606. DOI**:** 10.1021/ic901986w
20. Hohloch S, Pankhurst JR, Jaekel EE, Parker BF, Lussier DJ, Garner ME, Booth CH, Love JB, Arnold J (2017) Benzoquinonoid-bridged dinuclear actinide complexes. Dalton Trans Int Ed 46: 11615−11625. DOI:10.1039/C7DT02728A
21. Mills DP, Moro F, McMa ster J, van Slageren J, Lewis W, Blake AJ, Liddle STA (2011) Delocalized Arene-Bridged Diuranium Single-Molecule Magnet. Nat Chem 3: 454–460. DOI: 10.1038/NCHEM.1028
22. Døssing A (2014) Recent advances in the coordination chemistry of hydroxo-bridged complexes. Coord Chem Rev 280: 38–53. DOI: 10.1016/j.ccr.2014.08.005.
23. Neese F (2009) Prediction of molecular properties and molecular spectroscopy with density functional theory: From fundamental theory to exchange coupling. Coord Chem Rev 253: 526−563. DOI:10.1016/j.ccr.2008.05.014
24. Gryaznov D, Heifets E, Sedmidubsky D (2010) Density functional theory calculations on magnetic properties of actinide compounds. Phys Chem Chem Phys 12: 12273–12278. DOI: 10.1039/C0CP00372G.
25. Reta D, Ortu F, Randall S, Mills DP, Chilton NF, Winpenny REP, Natrajan L, Edwards B, Kaltsoyannis N (2018) The performance of density functional theory for the description of ground and excited state properties of inorganic and organometallic uranium compounds. J Organomet Chem 857: 58–74. DOI: 10.1016/j.jorganchem.2017.09.021
26. Becke AD (1993) Density-functional thermochemistry. III. The role of exact exchange. J Chem Phys 98: 5648. DOI: 10.1063/1.464913

27. Lee C, Yang W, Parr RG (1988) Development of the Colle-Salvetti correlation-energy formula into a functional of the electron density. Phys Rev B: Condens Matter Mater Phys 37: 785. DOI: 10.1103/PhysRevB.37.785

28. Noodleman LJ, Davidson ER (1986) Ligand spin polarization and antiferromagnetic coupling in transition metal dimers. J Chem Phys 109: 131–143. DOI: 10.1016/0301-0104(86)80192-6

29. Noodleman LJ, Peng CY, Case DA, Mouesca JM (1995) Orbital interactions, electron localization and spin coupling in iron-sulfur clusters. Coord Chem Rev 144: 199–244. DOI: 10.1016/0010-8545(95)07011-L

30. Spencer LP, Schelter EJ, Yang P, Gdula RL, Scott BL, Thompson JD, Kiplinger JL, Batista ER, Boncella JM (2009) Cation-cation interactions, magnetic communication, and reactivity of the pentavalent uranium ion $[U(NtBu)_2]^+$. Angew Chem Int Ed 48: 3795–3798. DOI: 10.1002/anie.200806190

31. Páez-Hernández D, Murillo-López JA, Arratia-Pérez R (2012) Optical and Magnetic Properties of the Complex Bis(dicyclooctatetraenyl)diuranium. A Theoretical View. Organometallics 31: 6297−6304. DOI: 10.1021/om300560h

32. Meskaldji S, Belkhiri A, Belkhiri L, Boucekkine A, Ephritikhine M (2012) Magnetic exchange coupling in imido bimetallic uranium(V) complexes. A relativistic DFT study. C R Chimie 15: 184–191. DOI:10.1016/j.crci.2011.07.006.

33. Meskaldji S, Zaiter A, Belkhiri L, Boucekkine A (2012) A relativistic DFT study of magnetic exchange coupling in ketimide bimetallic uranium(IV) complexes. Theor Chem Acc 131: 1151. DOI 10.1007/s00214-012-1151-9.

34. Teyar B, Belkhiri L, Costuas K, Boucekkine A, Meyer K (2016) Electronic Structure and Magnetic Properties of Dioxo-Bridged Diuranium Complexes with Diamond-Core Structural Motifs: A Relativistic DFT Study. Inorg Chem 55: 2870–2881. DOI**:** 10.1021/acs.inorgchem.5b02704

35. Teyar B, Boucenina S, Belkhiri L, Le Guennic B, Boucekkine A, Mazzanti M (2019) Theoretical Investigation of the Electronic Structure and Magnetic Properties of Oxo-Bridged Uranyl(V) Dinuclear and Trinuclear Complexes. Inorg Chem 58, 15: 10097-10110. https://doi.org/10.1021/acs.inorgchem.9b01237

36. Rosen RK, Andersen RA, Edelstein NMJ (1990) $[(MeC_5H_4)_3U]_2[(\mu\text{-}1,4\text{-}N_2C_6H_4)$: a bimetallic molecule with antiferromagnetic coupling between the uranium centers. J Am Chem Soc 112: 4588–4590. https://doi.org/10.1021/ja00167a092

37. Rosen RK (1989) Reaction of Tris(cyclopentadienyl)uranium compounds with amines, azides, and related ligands. Thesis of dissertation, California. https://digital.library.unt.edu/ark:/67531/metadc1451039/

38. te Velde G, Bickelhaupt FM, Baerends EJ, Fonseca Guerra C, van Gisbergen, SJA, Snijder JG, Ziegler T (2001) *Chemistry with ADF*. J Comput Chem 22: 931-967. https://doi.org/10.1002/jcc.1056
39. ADF 2019.302, SCM, Theoretical Chemistry, Vrije Universiteit, Amsterdam, The Netherlands, http://www.scm.com.
40. van Lenthe E, Baerends EJ, Snijders JG (1993) Relativistic regular two-component Hamiltonians. J Chem Phys 99: 4597-4610. https://doi.org/10.1063/1.466059
41. van Lenthe E, Ehlers AE, Baerends EJ (1999) Geometry optimization in the Zero Order Regular Approximation for relativistic effects, J Chem Phys 110: 8943-8953. https://doi.org/10.1063/1.478813
42. Becke AD (1988) Density-functional exchange-energy approximation with correct asymptotic behaviour. J Phys Rev A, General Physics 38: 3098−3100. https://doi.org/10.1103/PhysRevA.38.3098.
43. Perdew JP (1986) Density-functional approximation for the correlation energy of the inhomogeneous electron gas. Phys Rev B 33: 8822−8824. https://doi.org/10.1103/PhysRevB.33.8822
44. Perdew JP, Wang Y (1992) Accurate and simple analytic representation of the electron-gas correlation energy. Phys Rev B 45: 13244-13249. https://doi.org/10.1103/PhysRevB.45.13244
45. Gaunt AJ, Reilly SD, Enriquez AE, Scott BL, Ibers JA, Sekar P, Ingram KIM, Kaltsoyannis N, Neu MP (2008) Experimental and Theoretical Comparison of Actinide and Lanthanide Bonding in $M[N(EPR_2)_2]_3$ Complexes (M = U, Pu, La, Ce; E = S, Se, Te; R = Ph, ^{i}Pr, H). Inorg Chem 47: 29−41. https://doi.org/10.1021/ic701618a
46. Graves CR, Yang P, Kozimor SA, Vaughn AE, Clark DL, Conradson SD, Schelter EJ, Scott BL, Thompson JD, Hay PJ, Morris DE, Kiplinger JL (2008) Organometallic Uranium(V)−Imido Halide Complexes: From Synthesis to Electronic Structure and Bonding. J Am Chem Soc 130(15): 5272–5285 https://doi.org/10.1021/ja711010h
47. Becke AD (1993) Density-functional thermochemistry. III. The role of exact exchange. J Chem Phys 98: 5648. https://doi.org/10.1063/1.464913
48. Lee C, Yang W, Parr RG (1988) Development of the Colle-Salvetti correlation-energy formula into a functional of the electron density. Phys Rev B 37: 785. https://doi.org/10.1103/PhysRevB.37.785
49. Perdew JP, Burke K, Ernzerhof M (1996) Rationale for mixing exact exchange with density functional approximations. J Chem Phys 105: 9982. https://doi.org/10.1063/1.472933

50. Elkechai A, Belkhiri L, Amarouche M, Clappe C, Boucekkine A, Hauchard D, Ephritikhine M (2009) A DFT and experimental investigation of the electron affinity of the triscyclopentadienyl uranium complexes Cp_3UX. Dalton Trans Int Ed 2843-2849. https://doi.org/10.1039/b820873e
51. Zhekova H, Seth M, Ziegler T (2011) Introduction of a New Theory for the Calculation of Magnetic Coupling Based on Spin–Flip Constricted Variational Density Functional Theory. Application to Trinuclear Copper Complexes which Model the Native Intermediate in Multicopper Oxidases. J Chem Theory Comput 7: 1858–1866. https://doi.org/10.1021/ct200141v
52. Ciofini I, Daul CA (2003) DFT calculations of molecular magnetic properties of coordination compounds. Coord Chem Rev 238−239: 187−209. https://doi.org/10.1016/s0010-8545(02)00330-2
53. Selmi W, Abdelhak J, Marchivie M, Chastanet G, Zid MF(2017) An investigation by DFT of the electronic structure and magnetic properties of a novel l-oxo-iron(III) complex with the 1,10-phenathroline ligand. J Polyhedron 123: 441–452. https://doi.org/10.1016/j.poly.2016.12.012
54. Schultz NE, Zhao Y, Truhlar DG (2005) Density Functionals for Inorganometallic and Organometallic Chemistry. J Phys Chem A 109: 11127−11143. https://doi.org/10.1021/jp0539223.
55. Onishi T, Yamaki D, Yamaguchi K, Takano Y (2003) Theoretical calculations of effective exchange integrals by spin projected and unprojected broken-symmetry methods. I. Cluster models of K_2NiF_4-type solids. J Chem Phys 118: 9747−9761. https://doi.org/10.1063/1.1567251
56. Ruiz E, Cano J, Alvarez S, Alemany P (1999) Broken symmetry approach to calculation of exchange coupling constants for homobinuclear and heterobinuclear transition metal complexes. J Comp Chem 20: 1391-1400. https://doi.org/10.1002/(sici)1096-987x(199910)20:13<1391::aid-jcc6>3.0.co;2-j
57. Moreira IdPR, Costa R, Filatov M, Illas F (2007) Restricted Ensemble-Referenced Kohn−Sham versus Broken Symmetry Approaches in Density Functional Theory: Magnetic Coupling in Cu Binuclear Complexes. J Chem Theory Comput 3: 764–774. https://doi.org/10.1021/ct7000057
58. Graves CR, Yang P, Kozimor SA, Vaughn AE, Clark DL, Conradson SD, Schelter EJ, Scott BL, Thompson JD, Hay PJ, Morris DE, Kiplinger JL (2008) Organometallic Uranium(V)-Imido Halide Complexes: From Synthesis to Electronic Structure and Bonding. J Am Chem Soc 130: 5272–5285. https://doi.org/10.1021/ja711010h
59. Brennan JG, Andersen RA (1985) Electron-transfer reactions of trivalent uranium. Preparation and structure of the uranium metallocene compounds (MeC5H4)3U:NPh and $[(MeC_5H_4)_3U]_2$[.mu.-.eta.1,.eta.2-PhNCO]. J Am Chem Soc 107: 514–516. https://doi.org/10.1021/ja00288a047
60. Belkhiri L, Lissillour R, Boucekkine A (2005) The actinide–imide bonding revisited: A relativistic DFT study. J Mol Struct (theochem) 757: 155-164. https://doi.org/10.1016/j.theochem.2005.09.022

61. Reed AE, Curtiss LA, Weinhold F (1988) Intermolecular interactions from a natural bond orbital, donor-acceptor viewpoint. Chem Rev 88: 899-926. https://doi.org/10.1021/cr00088a005
62. Mayer I (1983) Charge, bond order and valence in the ab initio SCF theory. Chem Phys Lett 97: 270-274. https://doi.org/10.1016/0009-2614(83)80005-0
63. Nalewajski RF, Mrozek J (1994) Modified valence indices from the two-particle density matrix. Int J Quantum Chem 51: 187-200. https://doi.org/10.1002/qua.560510403
64. Nalewajski RF, Mrozek J, Michalak A (1997) Two-electron valence indices from the Kohn-Sham orbitals. Int J Quantum Chem 61: 589-601. https://doi.org/10.1002/(sici)1097-461x(1997)61:3<589::aid-qua28>3.0.co;2-2
65. Mulliken RS (1955) Electronic Population Analysis on LCAO-MO Molecular Wave Functions. I. J Chem Phys 23: 1833-1840. http://doi.org/10.1063/1.1740588
66. Wu H, Wu QY, Wang CZ, Lan JH, Liu ZR, Chai ZF, Shi WQ (2016) New insights into the selectivity of four 1,10-phenanthroline-derived ligands toward the separation of trivalent actinides and lanthanides: a DFT based comparison study. Dalton Trans. Int Ed 2016, 45, 8107–8117. https://doi.org/10.1039/c6dt00296j
67. Jones MB, Gaunt AJ, Gordon JC, Kaltsoyannis N, Neu MP, Scott BL (2013) Uncovering f-element bonding di□erences and electronic structure in a series of 1:3 and 1:4 complexes with a diselenophosphinate ligand. Chem Sci 4:1189-1203. https://doi.org/10.1039/c2sc21806b
68. Berryman VEJ, Whalley ZJ, Shephard JJ, Ochiai T, Price AN, Arnold PL, Parsons S, Kaltsoyannis N (2019) Computational analysis of M–O covalency in $M(OC_6H_5)_4$ (M = Ti, Zr, Hf, Ce, Th, U). Dalton Trans Int Ed 48: 2939-2947. https://doi.org/10.1039/c8dt05094e
69. Schelter EJ, Veauthier JM., Graves CR, John KD, Scott BL, Thompson JD, Pool-Davis-Tournear JA, Morris DE, Kiplinger JL (2008) 1,4-dicyanobenzene as a scaffold for the preparation of bimetallic actinide complexes exhibiting metal-metal communication. J Chem Eur 14: 7782–7790. https://doi.org/10.1002/chem.200800585.
70. Myers AJ, Rungthanaphatsophon P, Behrle AC, Vilanova SP, Kelley SP, Lukens WW, Walensky JR (2018) Structure and properties of $[(4,6\text{-}^{t}Bu_2C_6H_2O)_2Se]_2An(THF)_2$, An = U, Np, and their reaction with p-benzoquinone. Chem Commun 54: 10435-10438. https://doi.org/10.1039/c8cc05244a
71. Kahn O (1993) Molecular Magnetism. VCH publishers, New York:,1-380. ISBN 1-56081-566-3
72. Swart M, van Duijnen PTh, Snijders JG (2001) A charge analysis derived from an atomic multipole expansion. J Comput Chem 22(1): 79-88. https://doi.org/10.1002/1096-987X(20010115)22:1<79::AID-JCC8>3.0.CO;2-B